CHALMERS
UNIVERSITY OF TECHNOLOGY

Surface integrity of machined electron beam melted Ti6Al4V alloy manufactured with different contour settings and heat treatment

Available online at www.sciencedirect.com

ScienceDirect

Procedia CIRP 87 (2020) 327–332

www.elsevier.com/locate/procedia

5th CIRP CSI 2020

Surface Integrity of Machined Electron Beam Melted Ti6Al4V Alloy Manufactured with Different Contour Settings and Heat Treatment

D. Mallipeddi[a*], T. Hajali[a], L-E. Rännar[b], A. Bergström[c], S. Hernandez[d], E. Strandh[e], L. Nyborg[a], P. Krajnik[a]

[a] *Department of Industrial and Materials Science, ChalmersUniversity of Technology, SE-41296 Gothenburg, Sweden*
[b] *Department of Quality Management and Mechanical Engineering, Mid Sweden University, SE-83125 Östersund, Sweden*
[c] *AIM Sweden AB, Lägervägen 13, SE-83256 Frösön, Sweden*
[d] *Department of Verification of Components and Materials, AB Sandvik Coromant, SE-81181 Sandviken, Sweden*
[e] *Powder Materials & Additive Manufacturing, Swerim AB, Isafjordsgatan 28 A, SE-16440 Kista, Sweden*

* Corresponding author. Tel.: +46 317721245; *E-mail address:* mdinesh@chalmers.se

Abstract

The powder-bed-fusion-based Electron Beam Melting (EBM) is rapidly gaining interest as a feasible process in the manufacturing industry for producing intricate Ti6Al4V components. However, there is still a challenge of reducing production time and optimizing surface roughness. One way to improve surface roughness is to optimize the melting strategy, i.e. contour setting. This not only influences the obtained surface topographical features, but also the production time. Most industrial applications require subtractive post processing (machining) to obtain a desired functional surface. This paper is concerned with analysing surface and subsurface in turning of Ti6Al4V alloy, manufactured by EBM using different contour settings. Also, the effect of subsequent heat treatment, i.e. Hot Isostatic Pressing (HIP) is studied. The results indicate that avoiding of contours require a machining allowance of 1 mm to obtain surface roughness of about 0.5 µm (S_a). In case of three and five contours the machining allowance can be reduced to 0.25 mm. Microstructural differences originating from the subsequent HIP operation show no effect on machinability. Tensile residual stresses are generated when reaching down to the heat effected zone of contour settings.

Peer-review under responsibility of the scientific committee of the 5th CIRP CSI 2020

Keywords: Electron Beam Melting (EBM); Contour settings; Machining Ti6Al4V; Surface integrity

1. Introduction

Additive Manufacturing (AM) is developing rapidly with respect to both the materials and equipment. The principle distinction of this technology in comparison to traditional machining operations is its feasibility to produce intricate components simply by joining/fusing material layers following a 3D (CAD) model [1]. In the recent past, many AM technologies have been developed and the most commonly used method for AM of metal is powder bed fusion (PBF). The most common PBF techniques are electron beam melting (EBM) and selective laser melting (SLM). The techniques have different advantages, but in this work, the focus is on EBM that is used industrially in several sectors such as medical and aerospace. Moreover, this technology was one of the pioneers in serial production for the material Ti6Al4V. In EBM, a high energy electron beam melts consecutive layers of metal powders under a highly controlled vacuum atmosphere. The high vacuum atmosphere is best suited for printing of reactive alloys like Ti [2]. Today, three commercial Ti grades (2-comercially pure, 5-Ti6Al4V and 23-Ti6Al4V ELI) are produced by the EBM process. However, grade 5 (Ti6Al4V) is

Peer-review under responsibility of the scientific committee of the 5th CIRP CSI 2020
10.1016/j.procir.2020.02.091

used in wider applications such as biomedical, automotive, chemical and aerospace and this is because of its low density and mechanical properties [3].

Over the last decade, EBM has been extensively investigated in view of manufacturing of components using Ti6Al4V alloy. Today, EBM is considered an efficient process which can produce complex near net-shapes with minimal internal defects [4]. However, the inherently high surface roughness obtained by EBM remains a challenge that needs to be optimized/addressed. Rafi et al. [5] performed a comparative study between SLM and EBM built Ti6Al4V parts. In that study, it was concluded that larger particle size powders adhering to the surface and thicker layers contribute to the rougher surface of EBM builds. Apart from those parameters, additional factors such as contour strategies (number of contours, spacing between each contour line and contour overlap area with hatch) also play an influential role in obtainable surface roughness. General understanding is that increasing the number of contours improves the surface quality, but at the same time leads to higher production cost. On the other hand, no-contour strategy reduces production time but generates a rougher surface. However, irrespective of EBM parameters employed, the achievable surface roughness is still in the range of tens of microns. This means that for most cases an additional post processing, machining/finishing operation is required to obtain a desired functional surface. Therefore, the optimal manufacturing scenario for minimizing the overall costs is to produce parts with no-contours and then employ a certain post-processing operation without sacrificing the surface integrity. However, there is a serious lack of demonstrative case studies and research papers about the surface integrity of machined, additive manufactured alloys, with different contour settings and applicable heat-treatments.

To address this issue, cylindrical specimens of Ti6Al4V alloy were built using three different contour strategies; no-contour, three-contour, five-contours. Then a detailed analysis was performed to understand how machining affects the obtained surface integrity characteristics, such as surface roughness, microstructure and residual stresses. In addition, the effect of heat treatment, i.e. HIP (process generally used to close the pores and internal defects) on machinability and thereby surface integrity was also studied.

2. Materials and experimental work

Cylindrical specimens of Ti6Al4V alloy with dimensions; 205 mm in height, 40 mm in diameter and with wall thickness of 6 mm were produced using Arcam Q20plus EBM machine at AIM Sweden. Six samples were produced for each contour settings; no contours, three contours and five contours. Standard settings for the beam (current, speed) was used for the contours and the theoretical width of the contour region, that is the distance from the outer contour to the inner one, for three contours is 0.63 mm and 0.99 mm for five contours, and taking the heat zone/width of the beam into account, the region was about 0.9 mm and 1.26 mm, respectively. Half of the specimens from each contour setting were HIP at Quintus Technologies. Standard manufacturing cycle for Ti6Al4V alloy included heating at 920° C for a holding period of 2 hours under the pressure of 100 MPa.

The longitudinal turning experiments were performed using Montfort's RNC 600 turning machine at Sandvik Coromant's facilities (Sandviken). Two different types of uncoated-carbide inserts were used; N123J2-0600 RO H13A and RCGX 10 T3 M0-AlH10 for turning; hereafter referred only as H13A and H10 respectively. The geometries of both the inserts are intended for finishing operation. Irrespective of the inserts the cutting parameters were fixed for all the tests as follows: cutting speed V_c = 120 m/min, feed rate F_n = 0.25 mm/rev and depth of cut a_p = 0.25 mm. These parameters were chosen based on the pre-trial tests. Flood cooling with an emulsion was employed during machining.

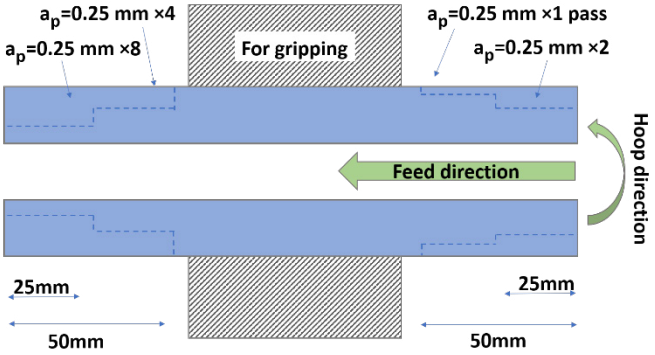

Fig. 1. Schematic illustration of a "stair-profile" cutting strategy for turn-finishing experiments.

To better understand the influence of contour settings, the experiments were executed using a "stair profile" strategy, shown in Fig. 1. Every sample was clamped in the middle to avoid/minimize vibrations. The first step comprised of a single 50 mm long cutting pass, followed by a 25 mm cutting pass to generate the second step. The sample was unclamped and turned around in order to machine the other side of the workpiece. The third step consisted of four consecutive cutting passes of 50 mm, followed by the fourth step of four more passes of 25 mm. In view of surface integrity studies in focus here, the first cutting step allows us to analyze the surface at approximately 0.25 mm depth, cutting step two at 0.5 mm, cutting step three at 1 mm and the final cutting step four at a depth of 2 mm. For illustration, refer to Fig. 1.

3. Characterization methods

Surface roughness was measured using Alicona InfiniteFocus SL 3D surface measurement system based on optical interferometry, which provides topological information utilizing the focus-variation technique. Two roughness-profile areas were measured for each condition from which the average value of roughness parameters was obtained. The measured area for as-built surfaces was around 2×9 mm and measurements were taken at 10x magnification. While, the measured area for machined surfaces was around 1×5 mm and measurements were taken at 20x magnification. The cylindrical form was removed by the software prior to the separation of waviness from roughness. All the data processing, filtering and

evolution of roughness parameters were performed according to ISO 25178 [6]. The following parameters were considered for the surface roughness analysis:

- S_a, average height of the selected area
- S_v, maximum valley depth of selected area
- S_{10Z}, ten-point height of the selected area

The microstructure of the turned surface was characterized by both light optical and scanning electron microscope (SEM). The light optical microscope used in this work was a Zeiss Axioscope7. The SEM instrument was LEO Gemini 1550 equipped with a field emission gun. The imaging was done at an acceleration voltage of 5 kV.

The residual stresses were measured by Xstress 3000G2R using Ti-Kα source. The lattice deformation for {110} α-Ti peak was measured and the stresses were determined by using standard $\sin^2(\psi)$ technique with five equi-$\sin^2$ (ψ) tilts ranging from -40/+40°.

4. Results and discussions

The surface finish of a component is of outmost importance as it has a significant influence on its functional performance. In this respect, the roughness of the as-built surfaces with different contour settings and their corresponding changes to subsequent finishing machining operation after each cutting step was examined. Although there are slight variations in the roughness values achieved after machining using two different inserts (H10 and H13A), the overall trends appear to be similar. The slight variations observed can be attributed to the existence of initial roughness variation of the two different builds produced with same contour settings. In other words, the initial surface condition of the same contour setting builds subjected to turning by two different inserts were different. The measured surface roughness values when using H13A insert are presented in Fig. 2. In as-built condition, the no-contour builds have two times higher values of surface roughness for all three analysed surface parameters compared to three and five contour builds. This is of no surprise as builds made with no contours are expected to be the roughest. Interestingly, there is no significant difference in roughness values between three contours and five contours settings. On the other hand, however, avoiding contours is beneficial in terms of production time; up to 20% reduction is attainable. For all the cases, HIP slightly improved the surface finish. For three and five contour setting builds, irrespective of the HIP condition, the S_a parameter which is the most common roughness parameter used for base line comparison has reduced/reached to ≤ 0.5 µm already after the first cut (i.e. removing 0.25 mm). Surprisingly, only for five contour-HIP condition, S_a value increased again to around 2 µm after cutting step 4 (i.e. cutting down to 2 mm). Further detailed investigation is needed to understand the reason for the observed increase in roughness. Whereas, for no-contour builds, the same level of smoothness, i.e. lower S_a values of around 0.5 µm were obtained only after second cutting step for HIP condition and after the third cutting step (i.e. removing 1 mm of material) for non-HIP condition. This clearly demonstrates that HIP has a significant (positive) influence on the no-contour builds. Interestingly, though the peaks were eliminated, the maximum valley depth, i.e. S_v parameter values, for both the three and five contour builds, remain in the range of tens of microns after the first cutting step. This is in turn reflected on the S_{10Z} values which is the summation of the average of the heights of the five peaks and valleys. For no contours, the S_V and S_{10Z} parameter follow the same trend as S_a, i.e. the lowest values were obtained only after the third cutting step.

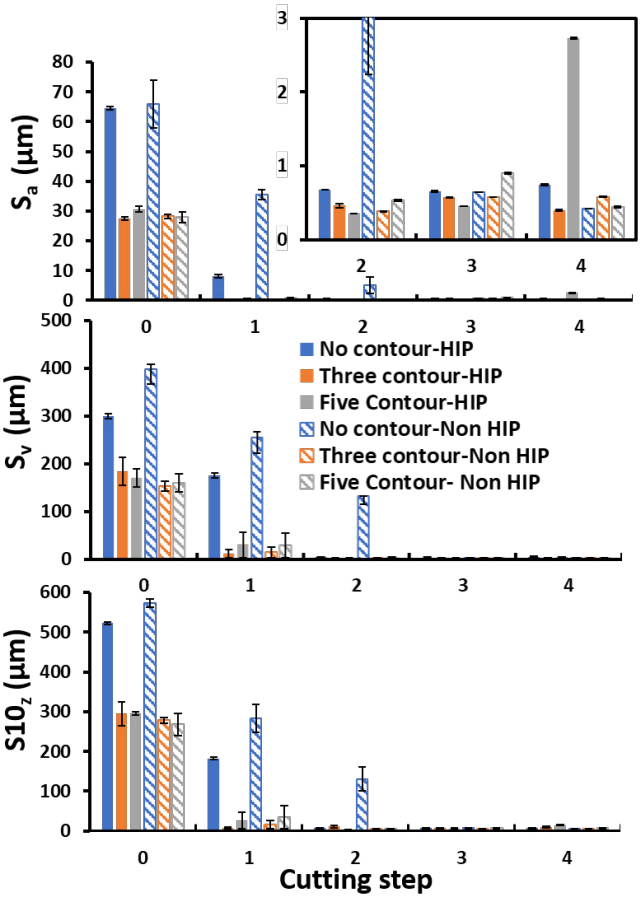

Fig. 2. Surface roughness S_a, S_v, and S_z of as-builds with different contour settings (presented as cutting step 0) and corresponding changes after turning using H13A insert. Note, the error bar indicates the maximum and minimum deviation of the mean value.

To summarize, the lowest values of (considered) surface roughness parameters (smoother surfaces) for no-contour builds were obtained after third cutting step, while for the three- and five-contours strategy required only two cutting steps. This has a significant implication on future process planning in terms of (required) machining allowance.

In addition to surface roughness measurements, the cross-sections were analyzed to check for any presence of surface irregularities between the three-contour setting builds. The analysis revealed open surface pores for all the conditions. However, these open pores extended to a depth of approx. 500 µm for no-contour builds, while for three- and five-contours they are confined to a layer of less than 150 µm. Probably this is a result of a circular periphery in combination with a hatch direction that alters 60 degrees in each layer. Using contours will "heal" the outer surface and close it, hence the rather deep open pores will turn into internal pores. HIP closed

these pores to a certain degree, but they were not eliminated completely.

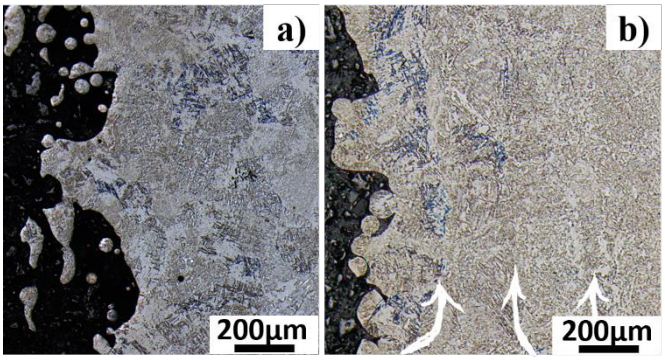

Fig. 3. Cross sections of as-built surfaces without HIP a) no-contour b) three-contours.

To illustrate the difference between contour and no-contour surfaces an exemplary image is shown in Fig. 3. Here, the contours from three-contour condition are clearly seen (indicated by the white arrows) in Fig. 3b. The distance between two adjacent contours is around 200 µm. This is true for both the three- and five-contours settings. For, three-contours, the theoretical width of the contour region, that is the distance from the outer contour to the inner contour is approximately 0.63 mm. But considering the effect of a heat zone and width of the beam the total region can extend to about 0.9 mm. Similarly, for five-contours settings, the theoretical width of the contour region is about 1 mm and considering the heat zone and width of the beam the extended region could be around 1.26 mm.

After machining, the cross-section of samples was analyzed for all the conditions and for each cutting step. Irrespective of the cutting insert used, the results showed that for no-contour builds these pores exist even after cutting step 2 i.e. after machining down to 0.5 mm (see Fig. 4 for details).

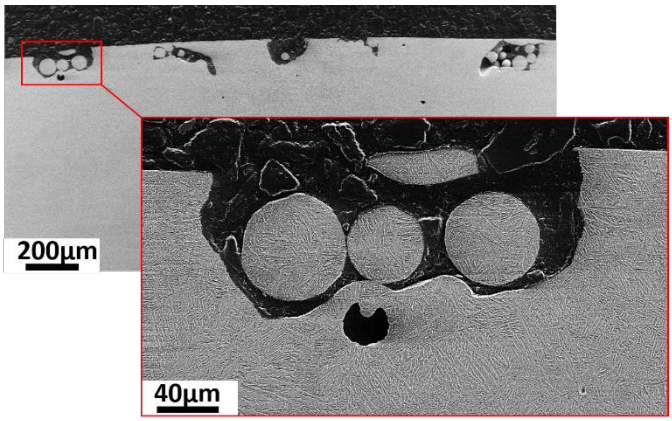

Fig. 4. Micrographs illustrating the presence of open pores or surface irregularities after cutting step 2 in no-contour and non HIP condition. The cutting insert used was H10.

The depth of these existing pores is around 100 µm. This is the case for the samples either with HIP or without HIP. While, after 3rd cutting step no such pores were observed indicating that for no contours the materials must be removed down to 1 mm to eliminate the surface irregularities/defects. In contrast, for the builds with contours no such pores or any sort of cracks were observed already after the first cutting step.

The microstructure of as-builds prior to HIP and after HIP is shown in Fig.5. The as-built microstructure consists of mixture of α+β phase within the columnar prior β grains parallel to the build direction. Also, the initial microstructure is very fine for all the builds irrespective of the contour settings. Note that the figures are taken in transverse/hoop direction and hence the columnar grains are not visible. Other studies reporting on similar microstructure attributed this finer microstructure to high solidification rates of an EBM process which generally are in the range of 10^3-10^5 K/s [7,8]. The coarsening of microstrutre took place after HIP. This happens as a result of the activated thermodynamic driving forces as the builds were exposed to elevated temperatures for longer times during HIP [9].

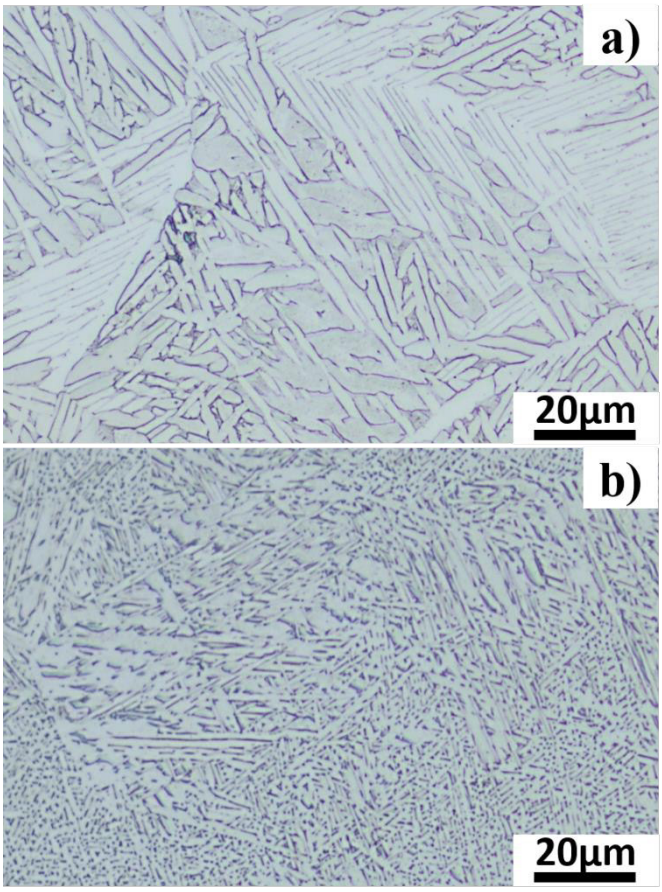

Fig. 5. As-built microstructure of no-contour build a) HIP b) Non HIP

Detailed examination at high magnification also revelead surface deformation towards the cutting direction. This is true for all the specimens regardless of the cutting insert. However, for contour builds, the plastic deformation of the surface was observed already after the first cutting step. But this deformation is confined to the outermost surface layer, see Fig. 6 for example. Here, no phase transformation was observed, indicating that the cutting temperature did not exceed the alloy transition temperature. Umbrello et.al [10] observed similar thin layer deformation after machining EBM-built Ti6Al4V (for non-HIP condition) under similar cutting conditions.

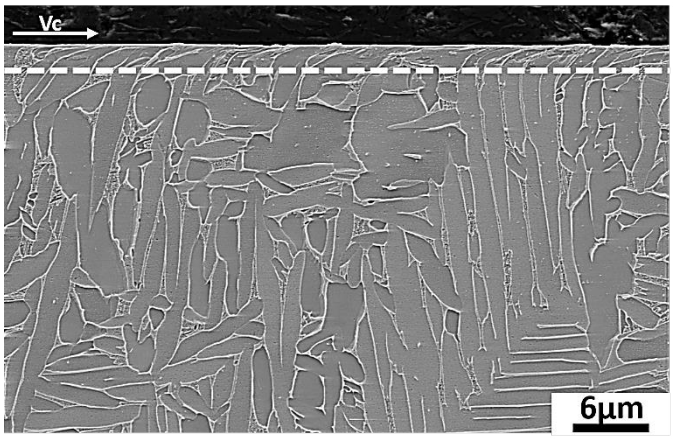

Fig. 6. Surface deformation observed in three-contour-HIP build after the second cutting step.

They also employed atomic force microscopy on the plastically deformed regions and confirmed decreased grain size and lamellae thickness. This might also be true in the present case scenario. However, detailed analysis needs to be performed for confirming this. Moreover, the surface deformation is similar for both HIP and non-HIP conditions that have different microstructures indicating that the variations in microstructure have no significant influence on the deformation behaviour.

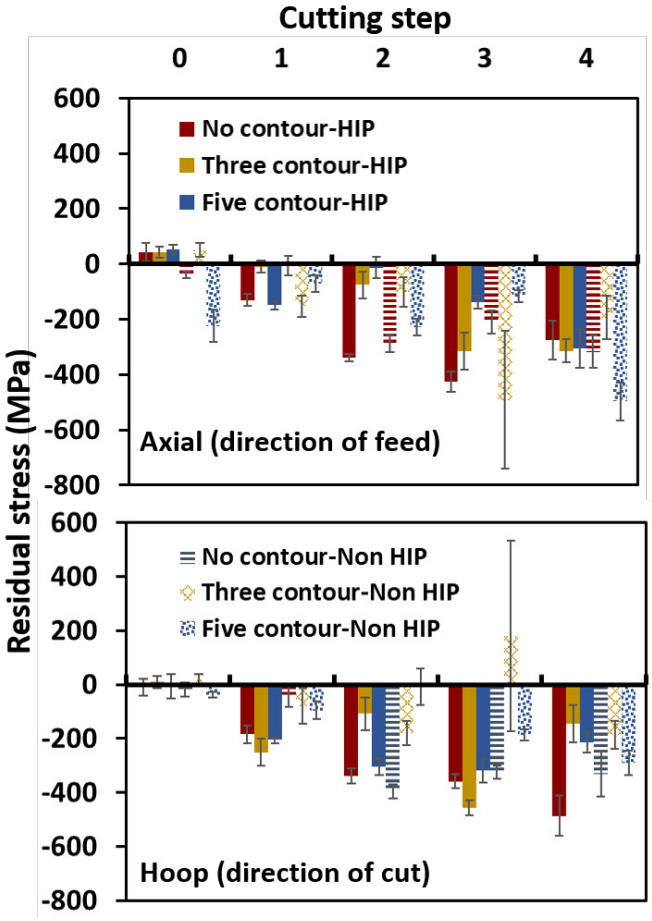

Fig. 7. Surface residual stresses after every cutting step of each specimen. Cutting step "0" refer to the virgin surface.

The other important aspect of surface integrity are residual stresses. It is well known that the compressive residual stresses are benificial, whereas tensile residual stresses are determental for both fatigue and corrosion resistance [11]. Therefore, it is vital to understand the stress states induced by machining after each cutting step. Here, regardless of the cutting insert used, similar trends of residual stress states were observed – hence only the machining results obtained using the H10 cutting insert are presented for discussion. The surface residual stresses were measured both in the axial (direction of feed/build) and hoop direction (direction of cut), see Fig.7. For all conditions, the residual stresses of virgin surface (referred to cutting step 0) were in tensile state with a magnitude of around 50 MPa. Note that the penetration depth of Ti-Kα source is around 6 µm, meaning that the measured stress values for virgin surface were only the average values of the peak summits. Hence, they should not be considered as absolute values, but are presented as a general reference for comparison. After machining, the residual stresses were in compressive state in both directions. However, the magnitude of the stresses varied between the directions, specimens and cutting steps. In general, the overall observed compressive stress trends are in line with the results reported by Bertolini et.al [12], who machined EBM-built Ti6Al4V alloy. The interesting observation in the present study is that only for three-contour and non-HIP condition after cutting step 3 (i.e. removing 1 mm of material), the residual stresses were tensile, particularly in the hoop direction. For the same condition, tough the stresses are in compressive state in axial direction the statistical error was large. This indicates some sense of inhomogeneity in the microstructure at around 1 mm depth which coincided with the width of the theoretical heat affected zone for 3-contour settings. To understand this nature of behaviour, a detailed local microstructural analysis needs to be performed in the future using diffraction techniques such as EBSD. On the other hand, such inhomogeneity developed due to countering might be eliminated via HIP process and hence no tensile stresses were observed. In the future, it would also be interesting to see what nature of stresses will be generated for five-contour samples when machined down to the surface that coincides with the heat affected zone.

5. Conclusions

In this paper, surface roughness, microstructure and residual stresses after machining EBM-built Ti6Al4V alloy with different contour strategies were investigated. A summary of the findings is provided below:

- EBM builds with no contours produced the roughest surface compared to three and five contour strategies. But at the same time no-contour strategy resulted in a reduction of AM production time by about 20%.
- For no-contour builds, the roughness of S_a less than 0.5 µm could be achieved after second cutting step for HIP condition. To achieve the same level of roughness, an additional cutting step was required for non-HIP condition. This indicates that the HIP process has a positive impact on surface roughness.

- When building a component with three and five contour settings, the S_a values of less than 0.5 µm were achieved after only one cutting pass. HIP process showed no influence when using contours.
- The deformation layer induced by machining was confined to the outermost surface layer. The microstructural difference originated from HIP had no influence on the obtained deformation.
- Turning operations induced compressive residual stresses for all tested conditions. However, tensile residual stresses are generated for three contour builds only after third cutting step, which coincides with the width of the heat-affected contour region.

Acknowledgements

This research was supported by Sweden's Innovation Agency (VINNOVA) Grant 2017-01265.

References

[1] Frazier WE. Metal aaditive manufacturing: A review. J Mater Eng Perform 2014; 23(6): 197-28.
[2] Wang P, Nai M, Tan X Vastola G, Raghavan S, Sin WJ, et al. Recent Progress of Additive Manufactured Ti-6Al-4V by Electron Beam Melting. Solid Free Fabr Proc 26th Annu Int 2016;691–704.
[3] Liu S, Shin YC. Additive manufacturing of Ti6Al4V alloy: A review. Mater Des 2019;164:107552.
[4] Zhang LC, Liu Y, Li S, Hao Y. Additive Manufacturing of Titanium Alloys by Electron Beam Melting: A Review. Adv Eng Mater. 2018;20(5):1–16.
[5] Rafi HK, Karthik N V., Gong H, Starr TL, Stucker BE. Microstructures and mechanical properties of Ti6Al4V parts fabricated by selective laser melting and electron beam melting. J Mater Eng Perform. 2013;22(12):3872–83.
[6] 25178-2:2012 I. Geometrical product specifications (GPS) - Surface texture: Areal - Part 2: Terms, definitions and surface texture parameters.
[7] Pushilina N, Syrtanov M, Kashkarov E, Murashkina T, Kudiiarov V, Laptev R, et al. Influence of manufacturing parameters on microstructure and hydrogen sorption behavior of electron beam melted titanium Ti-6Al-4V alloy. Materials 2018;11(5)
[8] Al-Bermani SS, Blackmore ML, Zhang W, Todd I. The origin of microstructural diversity, texture, and mechanical properties in electron beam melted Ti-6Al-4V. Metall Mater Trans A Phys Metall Mater Sci. 2010;41(13):3422–34.
[9] Ahlfors M, Bahbou F, Eklund A, Ackelid U. HIP for AM - Optimized Material Properties by HIP. Hot Isostatic Press HIP'17. 2019;10:1–10.
[10] Rotella G, Imbrogno S, Candamano S, Umbrello D. Surface integrity of machined additively manufactured Ti alloys. J Mater Process Technol. 2018;259:180–5
[11] Bertolini R, Bruschi S, Ghiotti A, Pezzato L, Dabalà M. Influence of the machining cooling strategies on the dental tribocorrosion behaviour of wrought and additive manufactured Ti6Al4V. Biotribology. 2017;11:60–8.
[12] Bertolini R, Lizzul L, Bruschi S, Ghiotti A. On the surface integrity of Electron Beam Melted Ti6Al4V after machining. Procedia CIRP 2019;82:326–31.